VIBRATION ANALYSIS OF THE MULTIPLE-HOLE MEMBRANE BY USING THE COUPLED DIEM-FE SCHEME

D.-S. Liu *

Department of Mechanical Engineering
National Chung Cheng University
Chiayi, Taiwan

Advanced Institute of Manufacturing with High-Tech Innovations
National Chung Cheng University
Chiayi, Taiwan

I.-H. Lin

Department of Mechanical Engineering
National Chung Cheng University
Chiayi, Taiwan

Advanced Institute of Manufacturing with High-Tech Innovations
National Chung Cheng University
Chiayi, Taiwan

ABSTRACT

This paper presents a 2D dynamics infinite element method (DIEM) for modeling the multiple-hole membrane for vibration analysis. A new concept involving converting the DIEM into a super element that can adjust the hole size and free and fixed boundary conditions around the hole is also proposed. The special element, embedded with an elastic membrane, is formulated on the basis of the conventional finite element method (FEM) by using the similarity mass/stiffness property of isoparametric elements and Craig-Bampton matrix reduction procedures. A DIEM-FE coupling scheme is also developed and self-programmed into the software MATLAB to conduct the vibration analysis of a membrane with multiple holes. The DIEM-FE approach is validated to study the vibration of the rectangular membranes by using the corresponding analytical solutions and the solutions obtained using the conventional FEM. The DIEM-FE is then applied to analyze imbedded L-shaped and circular opening problems. The effects of varying hole diameters and the free or fixed boundary condition along the hole are also examined. Finally, the last example shows that to perform vibration analysis of the multiple-hole membrane, only one DIEM mass/stiffness matrix must be calculated for all holes with an identical circular shape. Overall, this study provides a flexibility and efficient scheme for analyzing a wide variety of membrane vibration problems. The number of degrees of freedom and the corresponding PC memory storage are substantially reduced through the computation.

Keywords: Infinite element method, Finite element method, Craig-Bampton reduction method, Membrane vibration analysis.

1. INTRODUCTION

The vibration analysis of the membrane structure is a typical dynamic problem in various fields of engineering. The deformation of the membrane structure, caused by the vibration, leads to the destruction of the membrane structure in practical engineering. Because this problem is common, studying the vibration of the membrane structure and its dynamic response is a crucial scientific concern. The conventional finite element method (FEM) is commonly employed in such situations because it provides a convenient method to obtain the eigensolutions of membrane vibration. However, a large number of fine FEs are required and mesh modeling is generally tedious and complex. The hierarchical FEM [1-5] was developed to solve the vibration problems of membrane with arbitrary shapes including L-shape, triangle, the sectorial membrane, and the square membrane with a central circular opening. The nondimensional dynamic influence function method [6-9] based on the collocation method and nondimensional dynamic influence function was also proposed for the vibration analysis of arbitrarily shaped membranes. However, these methods require remeshing the model for analyzing different opening sizes in the same model.

The earlier works of infinite element method (IEM) are summarized in the literature [10,11]. In a series of related studies, Liu and Chiou [12-14] have discussed the recent developments in 2D and 3D IEMs. The conventional IEM approach was implemented using computer codes to solve the various types of classical elasticity and singularity problems. Liu, Chiou, and Chen [15-17] also extended the IEM to address elastostatic problems in which the constituent material properties were heterogeneous. Moreover, Liu, Zhuang, and Chung [18,19] and Liu, Fong, and Lin [20] have extended the IEM to address moisture diffusion in 2D and 3D problems, in which the constituent material

* Corresponding author (imedsl@ccu.edu.tw)

DOI : 10.1017/jmech.2015.60

Copyright © 2015 The Society of Theoretical and Applied Mechanics, R.O.C.
https://doi.org/10.1017/jmech.2015.60 Published online by Cambridge University Press

properties were heterogeneous. Liu, Tu, and Chung [21] discussed the eigenvalue problem of micro electro mechanical systems components and applied the displacement relationship between layers to solve the IEM formulations. In earlier works, the Guyan [22] reduction procedure was used to degenerate the mass/stiffness matrix of the FE domain. In dynamic analysis, however, the accuracy decreased because of the neglect of the inertial effect in the Guyan reduction procedure. The Craig-Bampton procedure [23] is well known as an ordinary and efficient method for analyzing the dynamics of large and complex structures.

This study adopts the Craig-Bampton procedure in the dynamic infinite element formulation to retain the accuracy of the IEM in dynamic analysis. The validity of the proposed approach is confirmed by comparing the results obtained by the vibration of a rectangular membrane with the analytical solutions and the solutions obtained using the conventional FEM. The applicability of the proposed method is then demonstrated by evaluating the relationship between the dynamic response and opening size of square membranes with a central circular opening.

2. OUT-OF-PLANE VIBRATION OF THE RECTANGULAR MEMBRANE

In this section, the governing equation is derived for solving the analytical solutions of membrane vibration problem. Consider a rectangular membrane extending over a domain D ($0 < x < a$, $0 < y < b$) and having a thickness h (Fig. 1). Assuming that the mass density ρ of the membrane is constant, the governing equation for the vibration of the membrane has the form shown in Eq. (1), where T is the tension force per unit length of the membrane edge. The Laplacian equation can be expressed in rectangular coordinates as shown in Eq. (2).

$$-T\nabla^2 W = \rho h \frac{\partial^2 W}{\partial t^2} \tag{1}$$

$$\nabla^2 = \frac{\partial^2}{\partial x^2} + \frac{\partial^2}{\partial y^2} \tag{2}$$

In addition, the boundary conditions at the fixed edges of the membrane have the forms shown in Eqs. (3) and (4).

$$W(0, y) = 0, \quad W(a, y) = 0 \tag{3}$$

$$W(x, 0) = 0, \quad W(x, b) = 0 \tag{4}$$

The differential equation and corresponding boundary conditions collectively constitute the eigenvalue problem. The solution of this eigenvalue problem consists of the eigenvalues $\beta_{m,n}$ and the natural frequency $\omega_{m,n}$, respectively.

$$\beta_{m,n} = \sqrt{\left[\left(\frac{m}{a}\right)^2 + \left(\frac{n}{b}\right)^2\right]} \quad m, n = 1, 2, \cdots \tag{5}$$

$$\omega_{m,n} = \pi \sqrt{\left[\left(\frac{m}{a}\right)^2 + \left(\frac{n}{b}\right)^2\right] \frac{T}{\rho h}} \tag{6}$$

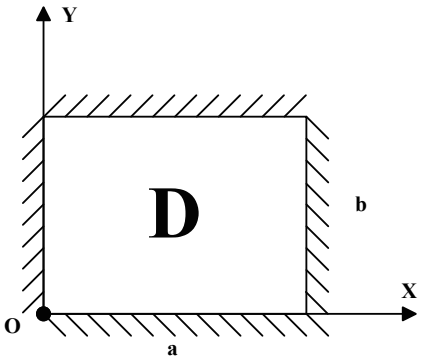


Fig. 1 Schematic illustration of rectangular membrane clamped at all four edges [21].

3. DYNAMIC INFINITE ELEMENT METHOD

3.1 Geometric Similarity of 2D Isoparametric Elements

In this section, the DIEM formulation is derived for modeling the membrane vibration problem. The basis of the proposed method is an IEM; the similar partition concept is the key to the IEM. This concept can be illustrated using the two similar general quadrilateral elements shown in Fig. 2.

For element I, the local nodes i are numbered 1, 2, 3, and 4 in counterclockwise direction. (x_i^I, y_i^I) denotes the global coordinate value of node i. By taking the global origin O and c as the center of the similarity and the proportionality ratio, respectively, element II is produced, of which the nodal coordinate value and length dimensions are similar to those of element I. The relationship between the corresponding nodes can be expressed as

$$(x_i^{II}, y_i^{II}) = (cx_i^I, cy_i^I) \tag{7}$$

where $c \in (0, 1)$ or $c \in (1, \infty)$, which implies the scale ratio. From the isoparametric representation, shape functions are used to express the coordinates of a point within element I in terms of the nodal coordinates. Thus, we have

$$x^I = \sum_{i=1}^{4} \phi_i x_i^I \tag{8}$$

$$y^I = \sum_{i=1}^{4} \phi_i y_i^I \tag{9}$$

Multiplying both sides by c and in view of Eq. (7),

$$x^{II} = cx^I = \sum \phi_i x_i^{II} \tag{10}$$

$$y^{II} = cy^I = \sum \phi_i y_i^{II} \tag{11}$$

From Eqs. (10) and (11), both quadrilateral elements II and I can be mapped using the same square-shaped master element, which is defined in natural coordinates. In other words, if one isoparametric element has coordinate node values similar to the values of other nodes, those elements are designated as similar elements.

https://doi.org/10.1017/jmech.2015.60 Published online by Cambridge University Press

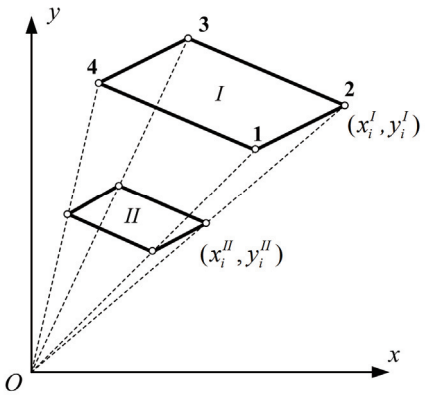


Fig. 2 Schematic diagram of similar four-node elements [10].

By mapping from the physical coordinates to the natural coordinates, the unit element matrix equation for the vibration of the membrane can be obtained from the governing differential equation, Eq. (1), by applying Galerkin's weighted residual approach. The resulting element matrix equation has the form

$$[M]\{\ddot{u}\}+[K]\{u\}=0 \tag{12}$$

Furthermore, the associated element mass/stiffness matrix are given by

$$[M^e]=\rho h\left\{\int_D \phi_i\,\phi_j\,\det[J]\,d\zeta\,d\eta\right\} \tag{13}$$

$$[K^e]=T\left\{\int_D \frac{\partial\phi_i}{\partial\zeta}\frac{\partial\phi_j}{\partial\zeta}\det[J]\,d\zeta\,d\eta+\int_D \frac{\partial\phi_i}{\partial\eta}\frac{\partial\phi_j}{\partial\eta}\det[J]\,d\zeta\,d\eta\right\} \tag{14}$$

in which

$$[J]=\begin{bmatrix}\dfrac{\partial x}{\partial\zeta} & \dfrac{\partial y}{\partial\zeta}\\ \dfrac{\partial x}{\partial\eta} & \dfrac{\partial y}{\partial\eta}\end{bmatrix}=\begin{bmatrix}\cdot & \cdot & \dfrac{\partial\phi_i}{\partial\zeta} & \cdot & \cdot\\ \cdot & \cdot & & \cdot & \cdot\\ \cdot & \cdot & \dfrac{\partial\phi_i}{\partial\eta} & \cdot & \cdot\end{bmatrix}\begin{bmatrix}\cdot & \cdot\\ \cdot & \cdot\\ x_i & y_i\\ \cdot & \cdot\\ \cdot & \cdot\end{bmatrix} \tag{15}$$

where $[J]$ is the Jacobian matrix of the transformation. Recalling Eq. (7) and from Eq. (15), we have

$$\det[J]^{II}=c^2\det[J]^{I} \tag{16}$$

Substituting Eq. (16) into Eqs. (13) and (14), we have

$$[M]^{II}=c^2[M]^{I} \tag{17}$$

$$[K]^{II}=[K]^{I} \tag{18}$$

3.2 Dynamic Infinite Element Formulation

This section presents the DIEM formulation for membrane vibration problems. The partition concept described in the previous section is shown in Fig. 3.

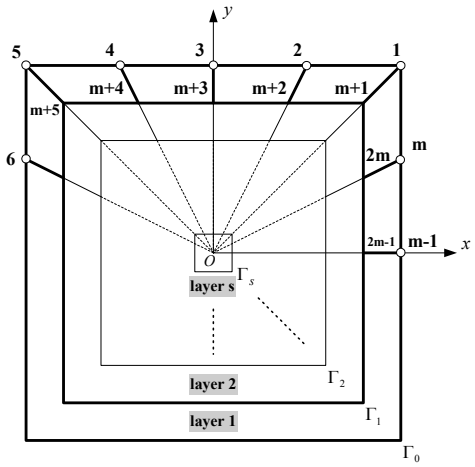


Fig. 3 Infinite element meshing scheme around reference point *O* [12].

The meshing steps are described as follows: first the outer boundary, Γ_0, is discretized with the total number of m master nodes, ordered in counterclockwise direction. Second, by choosing a similar partition center, *O*, and taking a constant $c \in (0, 1)$, similar curves Γ_1, Γ_2, …, Γ_s, … of Γ_0 are constructed with center *O* and proportionality constants c^1, c^2, …, c^s, …, respectively. The region bounded between Γ_{i-1} and Γ_i is called the *i*th layer (i = 1, 2, …, s), where s is the number of chosen layers. Third, each individual Γ_i is regularly discretized, the number of nodes and coordinates on each individual Γ_i can be determined from the master node coordinates with geometrically similar conditions. Fourth, every layer is auto-meshed into several four-node quadrilateral elements that are similar to one another from the layers in a radial direction. The total number of divided elements within one layer is m.

Considering the outermost layer, the element mass/stiffness matrix of each quadrilateral element can be calculated and assembled in an element-layer mass/stiffness matrix by using the conventional FE formulation. The mass/stiffness matrix of the first element-layer can be expressed as shown in Eqs. (19) and Eq. (20); Eq. (20) also shows the diagonal mass matrix, obtained from a lumped-mass formulation.

$$[K]^{I}=\begin{bmatrix}K_a & -A^T\\ -A & K_b\end{bmatrix}_{2m\times 2m} \tag{19}$$

$$[M]^{I}=\begin{bmatrix}M_a & -D^T\\ -D & M_b\end{bmatrix}_{2m\times 2m}=\begin{bmatrix}L_a & 0\\ 0 & L_b\end{bmatrix}_{2m\times 2m} \tag{20}$$

Recalling Eq. (12), the first layer eigenvalue formulation of the IEM can be expressed as shown in Eq. (21)

$$\left\{[K]^{I}-\lambda[M]^{I}\right\}\{u\}^{I}=0 \tag{21}$$

In the aforementioned equations, $\{u\}^I=\{\delta_0\ \ \delta_1\}^T$, where δ_0 denotes the outermost element layer's displacements of the IEM. The first element-layer as an eigenvalue formulation is shown in Eq. (22):

https://doi.org/10.1017/jmech.2015.60 Published online by Cambridge University Press

$$\left\{\begin{bmatrix} K_a & -A^T \\ -A & K_b \end{bmatrix} - \lambda \begin{bmatrix} L_a & 0 \\ 0 & L_b \end{bmatrix}\right\}\begin{Bmatrix} \delta_0 \\ \delta_1 \end{Bmatrix} = 0 \tag{22}$$

According to the foregoing similarity principle and consequent regular meshing rule, the mass/stiffness matrix of the s element-layers can be expressed as a set of algebraic equations, as follows:

$$\left\{\begin{bmatrix} K_a & -A^T \\ -A & K_b \end{bmatrix} - \lambda \begin{bmatrix} L_a & 0 \\ 0 & L_b \end{bmatrix}\right\}\begin{Bmatrix} \delta_0 \\ \delta_1 \end{Bmatrix} = 0 \quad \text{for layer 1} \tag{23}$$

$$\left\{\begin{bmatrix} K_a & -A^T \\ -A & K_b \end{bmatrix} - \lambda c^2 \begin{bmatrix} L_a & 0 \\ 0 & L_b \end{bmatrix}\right\}\begin{Bmatrix} \delta_1 \\ \delta_2 \end{Bmatrix} = 0 \quad \text{for layer 2} \tag{24}$$

$$\vdots$$

$$\left\{\begin{bmatrix} K_a & -A^T \\ -A & K_b \end{bmatrix} - \lambda c^{2(s-1)} \begin{bmatrix} L_a & 0 \\ 0 & L_b \end{bmatrix}\right\}\begin{Bmatrix} \delta_{s-1} \\ \delta_s \end{Bmatrix} = 0 \quad \text{for layer } s \tag{25}$$

By expanding and arranging the equations for all layers, adding the second equation for the i th element-layer and the first equation for the $(i+1)$ th element-layer, and letting $Q = K_b + K_a$, $R = L_b + c^2 L_a$, the following formulations are obtained.

$$\{K_a \delta_0 - A^T \delta_1\} - \lambda\{L_a \delta_0\} = 0 \tag{26}$$

$$\{-A\delta_0 + Q\delta_1 - A^T \delta_2\} - \lambda\{R\delta_1\} = 0 \tag{27}$$

$$\vdots$$

$$\{-A\delta_{i-1} + Q\delta_i - A^T \delta_{i+1}\} - \lambda c^{2(i-1)}\{R\delta_i\} = 0 \tag{28}$$

$$\vdots$$

$$\{-A\delta_{s-2} + Q\delta_{s-1} - A^T \delta_s\} - \lambda c^{2(s-2)}\{R\delta_{s-1}\} = 0 \tag{29}$$

$$\{-A\delta_{s-1} + K_b\delta_s\} - \lambda c^{2(s-1)}\{L_b\delta_s\} = 0 \tag{30}$$

The eigenvalue formulation of the IEM can be obtained by assembling the aforementioned equations.

$$\{[K]_{IEM} - \lambda[M]_{IEM}\}\{u\}_{IEM} = 0 \tag{31}$$

where

$$[K]_{IEM} = \begin{bmatrix} K_a & -A^T & 0 & 0 & 0 & 0 \\ -A & Q & -A^T & 0 & 0 & 0 \\ 0 & -A & Q & -A^T & 0 & 0 \\ 0 & 0 & 0 & \ddots & 0 & 0 \\ 0 & 0 & 0 & -A & Q & -A^T \\ 0 & 0 & 0 & 0 & -A & K_b \end{bmatrix} \tag{32}$$

$$[M]_{IEM} = \begin{bmatrix} L_a & 0 & 0 & 0 & 0 & 0 \\ 0 & R & 0 & 0 & 0 & 0 \\ 0 & 0 & c^2 R & 0 & 0 & 0 \\ 0 & 0 & 0 & \ddots & 0 & 0 \\ 0 & 0 & 0 & 0 & c^{2(s-2)} R & 0 \\ 0 & 0 & 0 & 0 & 0 & c^{2(s-1)} L_b \end{bmatrix} \tag{33}$$

$$\{u\}_{IEM} = \{\delta_0 \;\; \delta_1 \;\; \delta_2 \;\; \ldots \;\; \ldots \;\; \delta_{s-1} \;\; \delta_s\}^T \tag{34}$$

3.3 DIEM Coupled with the C-B Model Reduction Procedure

The present method condenses the internal displacements at a jointed boundary of two parts elements in the condensation process. The mass/stiffness matrix and displacement vector in the Eq. (31) can be partitioned as

$$[K]_{IEM} = \begin{bmatrix} K^{BB} & K^{BI} \\ K^{IB} & K^{II} \end{bmatrix} = \left[\begin{array}{c|ccccc} K_a & -A^T & 0 & 0 & 0 & 0 \\ \hline -A & Q & -A^T & 0 & 0 & 0 \\ 0 & -A & Q & -A^T & 0 & 0 \\ 0 & 0 & \ldots & \ldots & \ldots & 0 \\ 0 & 0 & 0 & -A & Q & -A^T \\ 0 & 0 & 0 & 0 & -A & K_b \end{array}\right] \tag{35}$$

$$[M]_{IEM} = \begin{bmatrix} M^{BB} & 0 \\ 0 & M^{II} \end{bmatrix} = \left[\begin{array}{c|ccccc} L_a & 0 & 0 & 0 & 0 & 0 \\ \hline 0 & R & 0 & 0 & 0 & 0 \\ 0 & 0 & c^2 R & 0 & 0 & 0 \\ 0 & 0 & 0 & \ddots & 0 & 0 \\ 0 & 0 & 0 & 0 & c^{2(s-2)} R & 0 \\ 0 & 0 & 0 & 0 & 0 & c^{2(s-1)} L_b \end{array}\right] \tag{36}$$

$$\{u\}_{IEM} = \begin{Bmatrix} u^B \\ u^I \end{Bmatrix} = \{\delta_0 \vdots \; \delta_1 \;\; \delta_2 \;\; \ldots \;\; \ldots \;\; \delta_{s-1} \;\; \delta_s\}^T \tag{37}$$

where the superscript B and I represent the boundary and interior nodes, respectively. The total set of degrees of freedoms (DOFs), u, is divided in the boundary DOFs, u^B, and internal DOFs, u^I. According to the Craig-Bampton reducing procedures, the coordinate transformation relating the infinite element domain final coordinate, p, to the IE domain initial coordinate, u, is

$$\{u\}_{IEM} = \begin{Bmatrix} u^B \\ u^I \end{Bmatrix} = \begin{bmatrix} I & 0 \\ \phi^C & \phi^N \end{bmatrix}\begin{Bmatrix} p^B \\ p^N \end{Bmatrix} = [\phi]\{p\}_{IEM}, \;\; p^B \equiv u^B \tag{38}$$

where ϕ^C represents the constrained modes of the IE subdomain, and ϕ^N represents the retained normal modes of the IE subdomain. The constrained modes are defined as the static deflection induced in the IE subdomain by imposing a unit displacement to one interface DOF while all other interface DOFs are fixed. The constrained modes can be calculated using Eq. (39).

$$\phi^C = -[K^{II}]^{-1}[K^{IB}] \tag{39}$$

https://doi.org/10.1017/jmech.2015.60 Published online by Cambridge University Press

The normal modes of the IE subdomain are calculated with all DOFs of the boundary held fixed. Thus, they are the eigenvectors of the eigenvalue problem, as in Eq. (40):

$$\left\{[K^{II}]-\lambda[M^{II}]\right\}\{u^{I}\}=0 \tag{40}$$

The normal modes of the IE subdomain are assumed normalized with respect to M^{II}, such that

$$[\phi^{II}]^{T}M^{II}[\phi^{II}]=I\ ,\ [\phi^{II}]^{T}K^{II}[\phi^{II}]=\Lambda\equiv\mathrm{diag}(\omega^{2}) \tag{41}$$

where ϕ^{II} is a matrix in which columns are the component normal modes. The normal set is usually truncated to a set of normal modes denoted by ϕ^{N}. In general, the retained normal modes must be derived using the complete mass/stiffness matrix first, and then the higher-order normal modes are truncated on the basis of the condition of the practical problem. Using the Lanczos procedure [24] can only calculate necessary component normal modes as retained normal modes without deriving the complete mass/stiffness matrix. By contrast, calculating the retained normal modes by using the Lanczos procedure can improve the computational efficiency.

Finally, the eigenvalue formulation of the IEM with the C-B reduced procedure can be obtained by substituting the coordinate transformation relation, Eq. (38), into Eq. (31) and premultiplying by the transpose of $[\phi]$.

$$\left\{[\phi]^{T}[K]_{IEM}[\phi]-\lambda[\phi]^{T}[M]_{IEM}[\phi]\right\}\{p\}_{IEM}=0 \tag{42}$$

Equation (42) can be expressed in the following concise form:

$$\left\{[\bar{K}]_{IEM}-\lambda[\bar{M}]_{IEM}\right\}\{\bar{p}\}_{IEM}=0 \tag{43}$$

where $[\bar{K}]_{IEM}$ and $[\bar{M}]_{IEM}$ denote the reduced mass/stiffness matrix and preserve the symmetrical characteristic of the global reduced mass/stiffness matrix in FE representation.

3.4 Implementation of the Coupled DIEM-FE Scheme

The DIEM is derived from the conventional FEM in space discretization. It employs the similarity characteristic of element mass/stiffness and the matrix condensing procedures to solve vibration problems in membrane structures. A series of layer-wise elements with similar shapes are virtually generated within the problem domain. The numerous resultant DOFs are condensed using Craig-Bampton reducing procedures. The nodes on the outer boundary of the DIEs are taken from interface common nodes between the DIE and FE subdomains. Because each DIE-reduced mass/stiffness matrix is pre-determined, the elements can be treated as regular FEs, and their DIE-reduced mass/stiffness matrices are assembled into the global combined mass/stiffness matrix. To illustrate the coupling algorithm, the assembling scheme is shown in Fig. 4. The global model is partitioned into two separate domains, which are separated from the coupling interface, Γ_0, namely Ω and D, modeled using the DIE and FE, respectively. For the conventional FEM, the algebraic-assembled element equations are derived from Eq. (12) and expressed as Eq. (44).

$$\left\{[K]_{FEM}-\lambda[M]_{FEM}\right\}\{u\}_{FEM}=0 \tag{44}$$

The global eigenvalue formulation can be expressed by assembling Eqs. (31) and (44).

$$\left\{\begin{bmatrix}K_{IEM} & 0\\ 0 & K_{FEM}\end{bmatrix}-\lambda\begin{bmatrix}M_{IEM} & 0\\ 0 & M_{FEM}\end{bmatrix}\right\}\begin{Bmatrix}\{u\}_{IEM}\\ \{u\}_{FEM}\end{Bmatrix}_{global}=0 \tag{45}$$

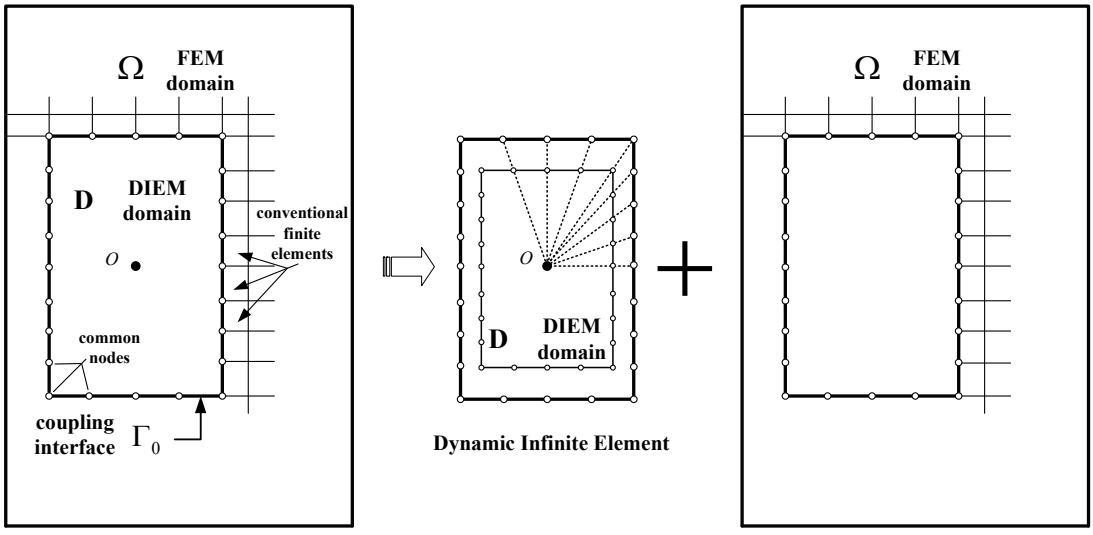


Fig. 4 Schematic diagram of DIE-FE coupling method.

https://doi.org/10.1017/jmech.2015.60 Published online by Cambridge University Press

According to Eq. (38), the coordinate transformation relating the final coordinate, p, to the initial coordinate, u, is

$$\begin{Bmatrix} \{u\}_{IEM} \\ \{u\}_{FEM} \end{Bmatrix}_{global} = \begin{bmatrix} \phi & 0 \\ 0 & I \end{bmatrix} \begin{Bmatrix} p_{IEM} \\ p_{FEM} \end{Bmatrix} = [\alpha]\{p\}_{global},$$
$$p_{FEM} \equiv u_{FEM} \tag{46}$$

The interface displacement along the IE domain must be equal to that of the FE domain based on the geometry compatibility; determining the transfer matrix β by simply forming $\{p\}_{global} = [\beta]\{q\}_{global}$ is convenient.

$$\{p\}_{global} = \begin{Bmatrix} p_{IEM} \\ p_{FEM} \end{Bmatrix} = \begin{Bmatrix} \begin{Bmatrix} p^B \\ p^N \end{Bmatrix}_{IEM} \\ \begin{Bmatrix} p^B \\ p^I \end{Bmatrix}_{FEM} \end{Bmatrix}$$
$$= \begin{bmatrix} I & 0 & 0 \\ 0 & 0 & I \\ I & 0 & 0 \\ 0 & I & 0 \end{bmatrix} \begin{Bmatrix} q^B \\ q^I \\ q^N \end{Bmatrix} = [\beta]\{q\}_{global},$$
$$p^B_{FEM} \equiv p^B_{IEM} \equiv q^B, \quad p^N \equiv q^N, \quad p^I \equiv q^I \tag{47}$$

By substituting Eq. (47) into Eq. (46), determining the transfer matrix S by simply forming $\{u\}_{global} = [S]\{q\}_{global}$ is convenient.

$$\{u\}_{global} = [\alpha]\{p\}_{global} = [\alpha][\beta]\{q\}_{global} = [S]\{q\}_{global}$$
$$[S] = \begin{bmatrix} I & 0 & 0 & 0 \\ \phi^C & \phi^N & 0 & 0 \\ 0 & 0 & I & 0 \\ 0 & 0 & 0 & I \end{bmatrix} \begin{bmatrix} I & 0 & 0 \\ 0 & 0 & I \\ I & 0 & 0 \\ 0 & I & 0 \end{bmatrix} = \begin{bmatrix} I & 0 & 0 \\ \phi^C & 0 & \phi^N \\ I & 0 & 0 \\ 0 & I & 0 \end{bmatrix} \tag{48}$$

Finally, the global eigenvalue formulation with the Craig-Bampton reduction procedure can be obtained by substituting the coordinate transformation relation, Eq. (48), into Eq. (45) and premultiplying by the transpose of $[S]$.

$$\left\{[S]^T[K]_{global}[S] - \lambda[S]^T[M]_{lglobal}[S]\right\}\{q\}_{global} = 0 \tag{49}$$

where

$$[\bar{K}]_{DIEM} = [S]^T[K]_{global}[S]$$
$$[\bar{M}]_{DIEM} = [S]^T[M]_{lglobal}[S] \tag{50}$$

where $[\bar{K}]_{DIEM}$ and $[\bar{M}]_{DIEM}$ denote the reduced mass/stiffness matrix and preserve the symmetry characteristic of the global reduced mass/stiffness matrix in FE representation. The related DIEM numerical procedures and coupled DIEM-FE scheme were programmed and executed using self-written codes in the MATLAB language [25]. In the proposed approach, the selective number of DOFs is substantially reduced, and hence the modeling and computational effort are substantially reduced.

When the problem domain includes multiple subdomains with repetitive geometry (*e.g.*, opening inclusions), employing FEs to model an entire domain with a large number of elements is not effective. Therefore, a DIEM-FE coupled scheme is proposed using only dynamic infinite elements to subdivide the entire domain into several subdomains without the use of FEs.

4. CASE STUDIES

To demonstrate the validity and performance of the proposed DIE-FEM, five examples are presented in this section. The first example is presented to verify the developed DIE-FE code by using the simply-supported rectangular membrane vibration problem; the results are compared with the analytical solutions. The second example employs the proposed method to solve the simply-supported L-shaped membrane vibration problem; for comparison purposes, results are also obtained from the FEM and the theoretically approximate solutions given by Fox *et al*. [26]. The third example applies the proposed method to determine the frequency parameter for a square membrane with a central circular opening. An extended study on the effect of the varied diameter of a central circular opening is presented in the fourth example. Finally, the fifth example applies the DIE-FE code to calculate the frequency parameter for a square membrane with multiple circular openings.

Example 1: Simply-Supported Rectangular Membrane

Consider a rectangular membrane, as shown in Fig. 1, with the following properties: a = 1.2m, b = 1m, thickness $h = 25 \times 10^{-6}$m, tension force per unit edge length T = 3300N/m, and mass density ρ = 2330kg/m^3. Assume that the membrane is rigidly clamped on all four sides. For comparison purposes, the results for the natural frequencies associated with the six lowest modes can be estimated using the linear theory of transversal vibrations for an elastic membrane (see Eq. (6)).

The DIE-FE coupling computational model, which is separated into two domains containing the FEM domain and the DIEM domain, is shown in Fig. 5. In the DIE-FE model, 64 interface nodes are used, and 224 four-node quadrilateral elements are used in the FE subdomain. The DIEM domain located in the center of the rectangular membrane and exhibiting a square shape has the same dimensions of length and width; w = 0.8m. The number of layers, s, is 50 and the proportionality constant, c, is 0.7 with respect to the related similar partition centers and ten retained modes for C-B reduction procedures. The material properties of the DIEM domain are identical to those in the FEM domain. The corresponding results obtained from the conventional FEM scheme are also presented. In the conventional FE model, the total number of elements is 480 and the total number of nodes is 525.

The graph comparing the lowest six natural frequencies from the theoretical solution and the proposed method solution are shown in Fig. 6, which also shows

https://doi.org/10.1017/jmech.2015.60 Published online by Cambridge University Press

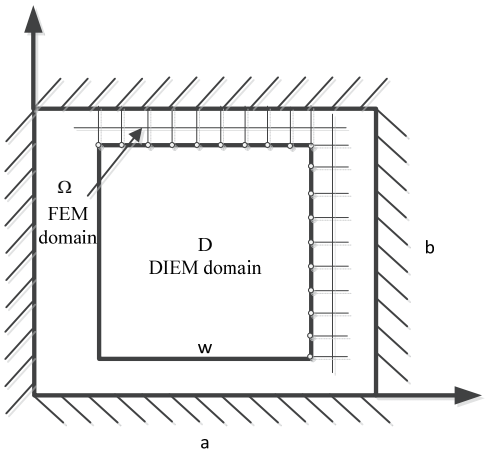


Fig. 5 DIE-FE Coupling computational model of rectangular membrane.

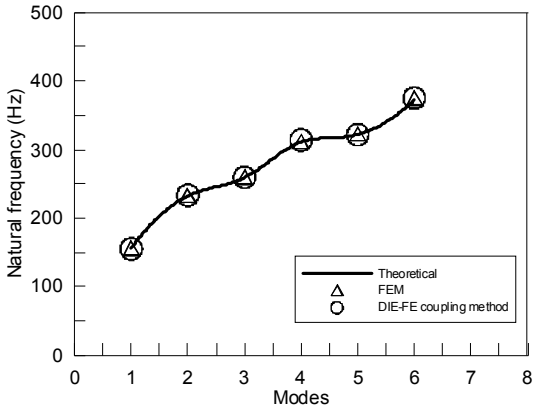


Fig. 6 The lowest 6 natural frequencies of rectangular membrane.

the results computed using the FEM. Comparing the sets of natural frequencies reveals that the DIE-FE results are in satisfactory agreement with the theoretical results.

Example 2: Simply-Supported L-Shaped Membrane

Consider an L-shaped membrane consisting of three identical squares and the same material properties as Example 1, as shown in Fig. 7. Assume that the membrane is rigidly clamped on all outer sides. There is no known analytical solution for this problem; however, highly accurate approximate solutions have been provided by Fox *et al*. [26].

Three types of mesh density are used to model the L-shaped membrane for comparison. In the conventional FE model, the total numbers of elements are 48, 75 and 108, the total numbers of nodes are 65, 96 and 133, and the corresponding numbers of system DOFs are 33, 56, and 85, respectively. In the DIE-FE model, 24, 32, and 40 interface nodes are used, and 28, 36, and 44 four-node quadrilateral elements are used in the FE subdomain, respectively. In the DIEM domain, the number of layers, *s*, is 50 and the proportionality constant, *c*, is 0.7 with respect to the related similar partition centers and ten retained modes for C-B reduction procedures. A DIE-FE coupling computational model with 40 interface nodes is shown in Fig. 8.

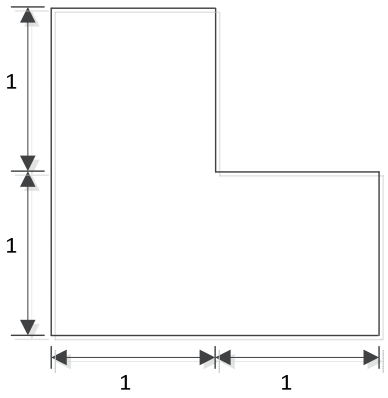


Fig. 7 The L-shaped membrane.

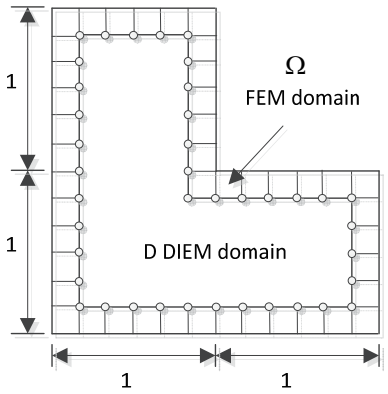


Fig. 8 DIE-FE Coupling computational model of L-shaped membrane.

The results for the ten lowest frequency parameters, $\Omega = \omega\sqrt{\rho / T}$, are shown in Table 1 with the solutions of Fox *et al*. [26]. To compare the results between the DIE (34) and FE (56). DIE (34) is substantially more accurate, although it has fewer system DOFs. The DIEM solutions are in favorable agreement with the solutions of Fox *et al*. [26].

Example 3: Simply-Supported Square Membrane with a Central Circular Opening

This example shows the applicability of the present method in modeling complex shapes. Consider a square membrane with a central circular opening and the same material properties as Example 1, as shown in Fig. 9. The membrane is supported along the internal and external boundaries.

The DIE-FE coupling computational model is shown in Fig. 10. In the DIE-FE model, 80 interface nodes are used, and 800 four-node quadrilateral elements are used in the FE subdomain. The DIEM domain, the gray part, located in the center of the square membrane and exhibiting a ring shape has the dimensions of an inner radius r = 0.4 and outer radius R = 0.5. The number of layers, s, is five and the proportionality constant, *c*, is 0.9564 with respect to the related similar partition centers and ten retained modes for C-B reduction procedures. The corresponding results obtained from the conventional FEM scheme are also presented. In the conventional FE model, the total number of

https://doi.org/10.1017/jmech.2015.60 Published online by Cambridge University Press

Table 1 Comparison of the frequency parameter for the 10 lowest modes of the simply supported L-shaped membrane. Numbers in parentheses denote the numbers of system degrees of freedom.

Method	Mode No.									
	1	2	3	4	5	6	7	8	9	10
FEM (33)	3.2087	4.0237	4.5878	5.7365	6.0321	7.0951	7.3876	7.6914	7.6914	8.2392
DIEM (34)	3.1573	4.0212	4.6311	5.6317	5.8871	6.6123	6.7012	6.9576	6.9869	7.5232
FEM (56)	3.1808	3.9881	4.5460	5.6402	5.9117	6.8740	7.1635	7.4709	7.4709	8.0035
DIEM (42)	3.1354	3.9655	4.5812	5.6491	5.8727	6.5427	6.6692	6.8464	7.0994	7.5554
FEM (85)	3.1654	3.9686	4.5234	5.5878	5.8453	6.7536	7.0375	7.3486	7.3486	7.8745
DIEM (50)	3.1237	3.9298	4.5385	5.6265	5.8521	6.5727	6.7909	6.9014	7.0061	7.5257
Fox *et al.* [26]	3.1048	3.8983	4.4428	5.4333	5.6492	6.4400	6.7043	7.0248	7.0248	7.5305

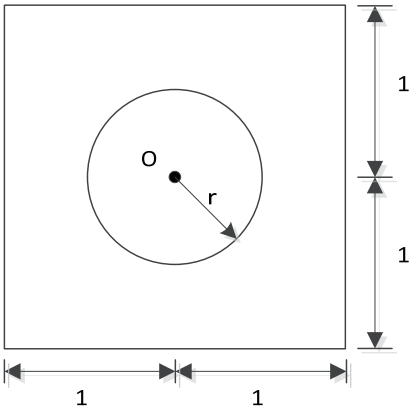


Fig. 9 The square membrane with a central circular opening.

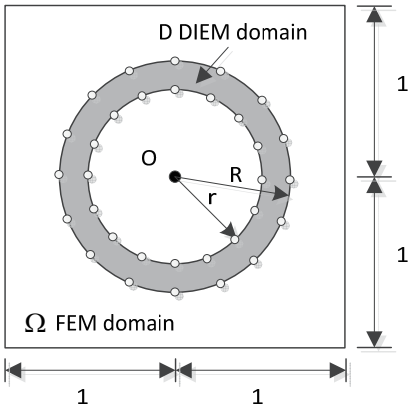


Fig. 10 DIE-FE Coupling computational model of the square membrane with a central circular opening.

elements is 1,152 and the total number of nodes is 1,248. Table 2 shows the results for the ten lowest frequency parameters with the solution of Houmat [5], and an accuracy up to 3 significant digits is reached. The DIEM solutions are in favorable agreement with the solutions of the conventional FE and Houmat [5].

Example 4: Effect of the Varied Diameter of a Central Circular Opening

In this section, an extended study of Example 3 for the effect of the varied diameter of a central circular opening is presented. Consider a square membrane with a central circular opening and the same material properties as Example 1, as shown in Fig. 9. In the DIE-FE model, 80 interface nodes are used, and 800 four-node quadrilateral elements are used in the FE subdomain. The dimension of the outer radius of the DIEM domain is $R = 0.5$, and the dimensions of the inner radius are 0.05, 0.10, 0.15, 0.20, 0.25, 0.30, 0.35, and 0.40. The number of layers is five and the proportionality constant with respect to the related similar partition centers is calculated using Eq. (51) and ten retained modes for C-B reduction procedures.

$$c = (r / R)^{1/s} \tag{51}$$

This example considers not only the varied dimension of the opening radius but also two types of boundary conditions; the inner boundary condition is free or fixed. The results of the ten lowest frequency parameters for the varied diameter of a central circular opening with a free or fixed inner boundary are presented in Table 3 and Table 4, respectively.

The example shows the flexibility of the present method in modeling the varied diameter of a circular opening. To investigate the effect of the varied diameter of a central circular opening in a conventional FEM, a new mass/stiffness matrix must be obtained by remeshing the model for each case. In the proposed DIE-FE coupling method, only the DIEM parameter, that is, the layers and proportionality constant, must be adjusted for calculating the new mass/stiffness matrix of the DIEM domain; it is not necessary to remesh the FE domain.

Example 5: Square Membrane with Multiple Identical Circular Openings

Consider a square membrane with multiple circular openings and the same material properties as Example 1.

https://doi.org/10.1017/jmech.2015.60 Published online by Cambridge University Press

Table 2 Comparison of the frequency parameter for the 10 lowest modes of the square membrane with a central circular opening.

Method	Mode No.									
	1	2	3	4	5	6	7	8	9	10
FEM	4.478	4.653	4.653	4.927	5.732	6.221	6.221	6.902	7.213	7.820
DIEM	4.476	4.652	4.652	4.928	5.730	6.222	6.222	6.907	7.217	7.829
Houmat, A. [5]	4.431	4.605	4.605	4.877	5.680	6.160	6.160	6.815	7.141	7.699

Table 3 The frequency parameter for the 10 lowest modes of the square membrane with a central circular opening (inner boundary condition is free).

Radius	Mode No.									
	1	2	3	4	5	6	7	8	9	10
0.05	2.248	3.516	3.516	4.462	4.948	4.974	5.692	5.692	6.436	6.436
0.10	2.272	3.455	3.455	4.470	4.987	5.102	5.659	5.659	6.351	6.351
0.15	2.314	3.372	3.372	4.464	4.974	5.272	5.625	5.625	6.312	6.312
0.20	2.371	3.295	3.295	4.435	4.927	5.463	5.624	5.624	6.344	6.344
0.25	2.445	3.237	3.237	4.382	4.845	5.644	5.644	5.671	6.428	6.428
0.30	2.536	3.209	3.209	4.308	4.744	5.657	5.657	5.881	6.552	6.552
0.35	2.646	3.216	3.216	4.229	4.652	5.640	5.640	6.080	6.709	6.709
0.40	2.778	3.260	3.260	4.160	4.589	5.590	5.590	6.245	6.898	6.898

Table 4 The frequency parameter for the 10 lowest modes of the square membrane with a central circular opening (inner boundary condition is fixed).

Radius	Mode No.									
	1	2	3	4	5	6	7	8	9	10
0.05	2.841	3.559	3.559	4.462	4.975	5.645	5.719	5.719	6.555	6.555
0.10	3.046	3.622	3.622	4.476	4.997	5.755	5.755	5.932	6.700	6.700
0.15	3.246	3.718	3.718	4.493	5.024	5.792	5.792	6.153	6.874	6.874
0.20	3.453	3.844	3.844	4.524	5.075	5.831	5.831	6.332	7.064	7.064
0.25	3.675	4.001	4.001	4.577	5.162	5.881	5.881	6.483	7.102	7.262
0.30	3.918	4.187	4.187	4.659	5.295	5.953	5.953	6.618	7.117	7.460
0.35	4.183	4.404	4.404	4.775	5.481	6.061	6.061	6.752	7.151	7.650
0.40	4.476	4.652	4.652	4.928	5.730	6.222	6.222	6.907	7.217	7.829

Figure 11 shows membrane models containing 1, 2, 3, and 4 identical circular openings. Five types of models are represented by (a) one circular opening on the corner, (b) two circular openings along one side, (c) two circular openings on the diagonal corner, (d) three circular openings along the corner, and (e) four circular openings with regular distribution. In the DIE-FE model, 48 interface nodes are used by each DIE, and 1,800, 1,584, 1,368, and 1,152 four-node quadrilateral elements are used by 1, 2, 3, and 4 identical circular openings in the FE subdomain. In the DIEM domain, the dimension of the inner radius $r = 0.1$ and outer radius $R = 0.25$; the number of layers is three and the proportionality constant is 0.7368 with respect to the related similar partition centers and ten retained modes for C-B reduction procedures. Table 5 shows the results for the ten lowest frequency parameters with the free inner boundary condition in five different models, and Table 6 shows the results for the ten lowest frequency parameters with the fixed inner boundary condition in five different models.

The example shows the efficiency of the present method in modeling multiple identical circular openings. To investigate the effect of multiple central circular openings in the proposed DIE-FE coupling method, the regions of openings are all replaced by DIEs such that only one DIEM mass/stiffness matrix requires calculation for all DIEs that have the same characteristics. Thus, the total number of DOFs in the computational model and the PC memory storage and processing requirements are considerably reduced.

https://doi.org/10.1017/jmech.2015.60 Published online by Cambridge University Press

Table 5 The frequency parameter for the 10 lowest modes of the square membrane with multiple identical circular openings (inner boundary condition is free).

Model	Mode No.									
	1	2	3	4	5	6	7	8	9	10
a	2.228	3.529	3.577	4.539	4.950	5.039	5.660	5.733	6.445	6.465
b	2.219	3.564	3.565	4.609	4.892	5.055	5.681	5.692	6.320	6.373
c	2.283	3.431	3.890	4.753	5.053	5.421	5.694	6.189	6.637	6.645
d	2.456	3.722	3.948	5.040	5.273	5.485	5.899	6.261	6.434	6.714
e	2.201	3.592	3.592	4.747	4.792	5.094	5.661	5.661	6.225	6.225

Table 6 The frequency parameter for the 10 lowest modes of the square membrane with multiple identical circular openings (inner boundary condition is fixed).

Model	Mode No.									
	1	2	3	4	5	6	7	8	9	10
a	2.402	3.551	3.913	4.817	5.065	5.331	5.766	6.491	6.611	6.621
b	2.567	3.835	4.142	5.116	5.349	5.372	6.379	6.656	6.701	6.994
c	2.695	3.967	4.440	5.157	5.284	5.981	6.202	6.599	6.832	6.921
d	3.345	4.474	4.706	5.523	5.834	6.156	6.741	6.926	7.153	7.260
e	3.136	4.642	4.642	5.245	5.936	6.849	6.849	6.926	7.243	7.243

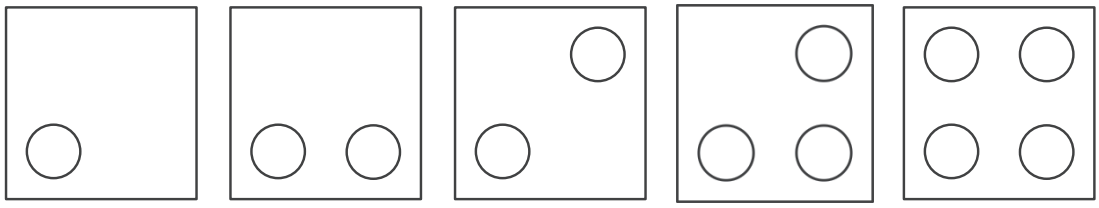


Fig. 11(a) ~ 11(e) Schematic illustration of the square membrane with multiple circular openings: (a) One circular opening on the corner; (b) Two circular openings along one side; (c) Two circular openings on the diagonal corner; (d) Three circular openings along the corner; (e) Four circular openings with regular distribution.

5. CONCLUSIONS

A sophisticated DIEM/FEM coupling algorithm based on the IEM designed to analyze the out-of-plane vibration response of membranes is developed in this study. A similarity-based partitioning method is used to generate a multilayered arrangement of infinitesimal elements positioned symmetrically around a central reference point in the IE domain. The individual element layers are then condensed to form a single IE super element by using C-B reduction procedures. The performance of the proposed DIE-FEM is validated by comparing the results obtained for the vibration of a rectangular membrane with the analytical solutions and the solutions obtained using the conventional FEM. The performance is also demonstrated by comparing the results obtained for the vibration of the L-shaped membrane with those of the solutions presented in literature. The flexibility of the present method for various dimensions of the radius in the square membrane with a central circular opening can be modeled without modifying the original model simply by controlling the parameters of layers and the proportionality constant within the DIE domain. Regarding the efficiency of the present method for investigating the effect of multiple circular openings, in the proposed DIE-FE coupling method, the regions of openings are all replaced by DIEs such that only one DIEM mass/stiffness matrix requires calculation for all DIEs that have the same characteristics. Thus, the total number of DOFs in the computational model and the PC memory storage and processing requirements are considerably reduced. Overall, the results presented in this study show that the proposed DIEM method provides a flexible and efficient means of predicting the effects of manufacturing design (*i.e.*, openings) on the dynamic response of membranes.

https://doi.org/10.1017/jmech.2015.60 Published online by Cambridge University Press

ACKNOWLEDGEMENTS

The current authors gratefully acknowledge the financial support provided to this study by the Ministry of Science and Technology, Taiwan, ROC, under Grant NO. MOST 103-2221-E-194-010-MY3 and NSC 101-2221-E-194-014-MY3.

REFERENCES

1. Houmat, A., "Hierarchical Finite Element Analysis of the Vibration of Membranes," *Journal of Sound and Vibration*, **201**, pp. 465–472 (1997).
2. Houmat, A., "A Triangular Fourier P-Element for the Analysis of Membrane Vibrations," *Journal of Sound and Vibration*, **230**, pp. 31–43 (2000).
3. Houmat, A., "A Sector Fourier P-Element for Free Vibration Analysis of Sectorial Membranes," *Computers & Structures*, **79**, pp. 1147–1152 (2001).
4. Houmat, A., "Free Vibration Analysis of Membranes Using the H-P Version of the Finite Element Method," *Journal of Sound and Vibration*, **282**, pp. 401–410 (2005).
5. Houmat, A., "Free Vibration Analysis of Arbitrarily Shaped Membranes Using the Trigonometric P-Version of the Finite-Element Method," *Thin-Walled Structures*, **44**, pp. 943–951 (2006).
6. Kang, S. W., Lee, J. M. and Kang, Y. J., "Vibration Analysis of Arbitrarily Shaped Membranes Using Non-Dimensional Dynamic Influence Function," *Journal of Sound and Vibration*, **221**, pp. 117–132 (1999).
7. Kang, S. W. and Lee, J. M., "Application of Free Vibration Analysis of Membranes Using the Non-Dimensional Dynamic Influence Function," *Journal of Sound and Vibration*, **234**, pp. 455–470 (2000).
8. Kang, S. W. and Lee, J. M., "Free Vibration Analysis of an Unsymmetric Trapezoidal Membrane," *Journal of Sound and Vibration*, **272**, pp. 450–460 (2004).
9. Kang, S. W., Atluri, S. N. and Kim, S. H., "Application of the Nondimensional Dynamic Influence Function Method for Free Vibration Analysis of Arbitrarily Shaped Membranes," *Journal of Vibration and Acoustics-Transactions of the ASME*, **134**, pp. 041008-1–041008-8 (2012).
10. Guo, Z. H., "Similar Isoparametric Elements," *Science Bulletin*, **24**, pp. 577–582 (1979).
11. Ying, L. A., "An Introduction to Infinite Element Method.," *Mathematics in Practice Theory*, **2**, pp. 69–78 (1992).
12. Liu, D. S. and Chiou, D. Y., "A Coupled IEM/FEM Approach for Solving Elastic Problems with Multiple Cracks," *International Journal of Solids and Structures*, **40**, pp. 1973–1993 (2003).
13. Liu, D. S., Chiou, D. Y. and Lin, C. H., "3D IEM Formulation with an IEM/FEM Coupling Scheme for Solving Elastostatic Problems," *Advances in Engineering Software*, **34**, pp. 309–320 (2003).
14. Liu, D. S. and Chiou, D. Y., "2-D Infinite Element Modeling for Elastostatic Problems with Geometric Singularity and Unbounded Domain," *Computers & Structures*, **83**, pp. 2086–2099 (2005).
15. Liu, D. S. and Chiou, D. Y., "Modeling of Inclusions with Interphases in Heterogeneous Material Using the Infinite Element Method," *Computational Materials Science*, **31**, pp. 405–420 (2004).
16. Liu, D. S., Chiou, D. Y. and Lin, C. H., "A Hybrid 3D Thermo-Elastic Infinite Element Modeling for Area-Array Package Solder Joints," *Finite Elements in Analysis and Design*, **40**, pp. 1703–1727 (2004).
17. Liu, D. S., Chen, C. Y. and Chiou, D. Y., "3-D Modeling of a Composite Material Reinforced with Multiple Thickly Coated Particles Using the Infinite Element Method," *CMES-Computer Modeling in Engineering & Sciences*, **9**, pp. 179–191 (2005).
18. Liu, D. S., Zhuang, Z. W., Chung, C. L. and Chen, C. Y., "Modeling of Moisture Diffusion in Heterogeneous Epoxy Resin Containing Multiple Randomly Distributed Particles Using Hybrid Moisture Element Method," *CMC-Computers Materials & Continua*, **13**, pp. 89–113 (2009).
19. Liu, D. S., Zhuang, Z. W., Lyu, S. R., Chung, C. L. and Lin, P. C., "Modeling of Moisture Diffusion in Permeable Fiber-Reinforced Polymer Composites Using Heterogeneous Hybrid Moisture Element Method," *CMC-Computers Materials & Continua*, **26**, pp. 111–136 (2011).
20. Liu, D. S., Fong, Z. H., Lin, I. H. and Zhuang, Z. W., "Modeling of Moisture Diffusion in Permeable Particle-Reinforced Epoxy Resins Using Three-Dimensional Heterogeneous Hybrid Moisture Element Method," *CMES-Computer Modeling in Engineering & Sciences*, **93**, pp. 441–468 (2013).
21. Liu, D. S., Tu, C. Y. and Chung, C. L., "Eigenvalue Analysis of Mems Components with Multi-Defect Using Infinite Element Method Algorithm," *CMC-Computers Materials & Continua*, **28**, pp. 97–120 (2012).
22. Guyan, R. J., "Reduction of Stiffness and Mass Matrices," *AIAA Journal*, **3**, pp. 380–380 (1965).
23. Bampton, M. C. C. and Craig, J. R. R., "Coupling of Substructures for Dynamic Analyses," *AIAA Journal*, **6**, pp. 1313–1319 (1968).
24. Bathe, K.-J., *Finite Element Procedures*, Klaus-Jurgen Bathe (2006).
25. Kwon, Y. W. and Bang, H., *The Finite Element Method Using Matlab*, CRC press, Boca Raton (2000).
26. Fox, L., Henrici, P. and Moler, C., "Approximations and Bounds for Eigenvalues of Elliptic Operators," *SIAM Journal on Numerical Analysis*, **4**, pp. 89–102 (1967).

(Manuscript received March 21, 2015,
accepted for publication June 2, 2015.)

https://doi.org/10.1017/jmech.2015.60 Published online by Cambridge University Press